Research Article Adv. Mater. Lett. 2015, **6**(1), 40-46 ADVANCED MATERIALS Letters

www.amlett.com, www.vbripress.com/aml, DOI: 10.5185/amlett.2015.amwc1194 Published online by the VBRI press in 2015

On the molecular basis of silica gel morphology

Agnieszka Kierys[1], Jacek Goworek[1], Michał Rawski[2], Istvan Halasz[3*]

[1]*M. Curie-Sklodowska Univ. Faculty of Chemistry, Department of Adsorption,*
M. Curie-Sklodowska Sq.3, 20031 Lublin, Poland
[2]*M. Curie-Sklodowska Univ., Faculty of Chemistry, Analytical Laboratory,*
Pl. M. Curie-Sklodowskiej Sq.3, 20031 Lublin, Poland
[3]*PQ Corporation, Research and Development Center, 280 Cedar Grove Road, Conshohocken, PA 19428 USA*

[*]Corresponding author. E-mail: istvan.halasz@pqcorp.com

Received: 14 July 2014, Revised: 25 September 2014 and Accepted: 24 October 2014

ABSTRACT

Distinction between molecular constitutions of differently made silica gels succeeded only recently. This paper seeks relationship between the different molecular structures of acid and base set gels and their morphology and pore structure. Gels were fabricated from both tetraethyl orthosilicate, TEOS, in organic solvent environment and from an economically more desirable, commercial, aqueous Na-silicate solution. When their gelling was performed in the pores of an organic resin, Amberlite, further molecular differences were observed, along with associated morphology and porosity differences. We present here unprecedented atomically resolved TEM pictures that visually prove that the molecular structures of gels deduced from their ^{29}Si NMR and Raman spectra are real, which could also be demonstrated by computer models. Copyright © 2015 VBRI Press.

Keywords: Silica gel; sodium silicate; TEOS; molecular structure; TEM; porosity.

Agnieszka Kierys is an Assistant Professor at the Adsorption Department of Maria Curie-Sklodowska University in Poland. She received her PhD in chemistry in 2010. She worked on projects concerning the thermal degradation of organic templates from ordered mesoporous materials, the investigation of adsorption-desorption mechanisms of alkanes by positron annihilation lifetime spectroscopy (PALS) and many other. Her current work focuses on the synthesis of new polymer-inorganic nanocomposites addressed to controlled drug release formulations and catalysis.

Jacek Goworek Born in Poland in 1949. After graduation from Institute of Chemistry MCS University in 1971, he was employed in the Department of Physical Chemistry. Currently he is head of Department of Adsorption. From 1993 to 1999 he was Vice-Dean of Chemistry Faculty. From 2002 to 2005 he was Vice-Dean for International Program Studies and International Relations of the Faculty of Chemistry. He published over 200 papers in international journals and monographs. Since 2005 – Vice-Dean for research of Faculty of Chemistry.

Istvan Halasz Obtained Ph.D. from the Hungarian Academy of Sciences (HAS) in 1982. In the Hungarian Hydrocarbon Research Institute he developed and scaled-up efficient processes for pharmaceutical, fine chemical and petrochemical industries. Later at the Chemistry Research Institute of HAS and at USA universities he studied zeolite catalysis, oxide superconductor synthesis, and catalytic fume abatement for automobile and stationary exhausts. In the past 16 years he has investigated the properties of silica and silicate derivatives at the Research & Development Center of PQ Corporation. He is member of several professional societies, chaired the Philadelphia Catalysis Club, was president of North-East Corridor Zeolite Association (NECZA). He edited a book on catalysis, and authored 110+ book chapters and papers, 7 patents, and 80+ conference presentations.

Introduction

Silica gels are widely used adsorbents, fillers, coatings, catalyst supports, etc. in a variety of technologies **[1-4]** and a number of new studies are underway for utilizing these versatile amorphous materials in optical, electronics, pharmaceutical and other advanced applications **[5-13]**. For a specific use most frequently their morphology and porosity are empirically adjusted to a desired value without even considering that maybe the adjustment affected their molecular constitution and this brought about the wanted physical properties. Except very few theoretical deductions **[3, 14]**, the molecular structures of different silica gels have been generally viewed as indistinguishably random mix of siloxane rings and chains hence have not even been investigated. Only in the past few years started publications appear that proved experimentally, mainly by Raman and ^{29}Si NMR studies, that differently made silica gels might possess distinctly different molecular structures **[15-18]** and this correlates with differences in some of their physical properties **[15, 19]**. In the present paper we provide new experimental evidence for distinct molecular constitutions of hydrated and dehydrated silica gels made at acidic and basic conditions and compare their molecular level differences with their morphology and porosity.

It has long been known that dehydration of a hydrogel can easily lead to sintering, which results in fractured structure and/or porosity loss, especially when the removal of water involves calcination at elevated temperatures. Therefore, a variety of precautious measures have been developed for the drying and calcination procedures, which can assure coherent structure with smooth surface and enough mechanical strength to maintain high surface area and pore volume for the ultimate xero- or aerogels **[2-4]**. A special, almost one century old route for making such stable, smooth and highly porous silica gels is their synthesis in the presence of other materials like carbon black, CO_2 or organic polymers, which do not react with the silica and can be removed from the stabilized gel by washing, high temperature firing, or other procedures **[4, 20, 21]**.

In the course of the past few years we have demonstrated that a mesoporous, moderately polar acrylic ester resin, Amberlite XAD7HP **[22]**, can be an excellent additive for making 550 ^{o}C hardened, porous silica via gels from tetraethyl orthosilicate, TEOS **[15, 19]**. The morphology and porosity of these materials were found to differ substantially and characteristically when made at acidic or basic pH values. In this paper we test the effect of Amberlite XAD7HP on acid and base set gels made from a commercially more viable aqueous Na-silicate solution and compare their physical properties with their molecular structures. This long suspected connection was first identified on TEOS based gels using mostly Raman and ^{29}Si NMR techniques for distinguishing their molecular assembly **[15]**. Using unprecedentedly high resolution transmission electron microscopic, TEM, pictures and molecular modeling techniques we visually ascertain here that the spectroscopic structural deductions are indeed viable.

Table 1. Selected properties of silica gels and their composites with Amberlite XAD7HP acrylic ester resin made from STAR sodium silicate solution (names with Na) or TEOS (names with T). S_{BET} = BET surface area; V_p = total pore volume; D1 and D2 = major mesopore diameters based on N_2 sorption data; nm = not measured.

Sample	Description	SBET [m^2g^{-1}]	Vp [cm^3g^{-1}]	D1 [nm]	D2 [nm]
S-1	Rinsed, dry XAD7HP support	486	0.670	3.8	8.8
Na-1	Sample **S-1** saturated with STAR solution	7.4	0.007	nm	nm
Na-2	Sample **Na-1** calcined at 560 ° C	3.6	0.003	nm	nm
Na-3A	Sample **Na-1** gelled at pH ~ 1; washed; dried at 80 ° C	510	0.36	3.9	-
Na-4A	Sample **Na-3A** calcined at 560 ° C	575	1.05	-	40
Na-3B	Sample **Na-1** gelled at pH ~ 7.4; washed; dried at 80 ° C	489	0.46	3.8	-
Na-4B	Sample **Na-3B** calcined at 560 ° C	nm	nm	nm	nm
S-2	Rinsed, dry XAD7HP support	498	0.68	3.8	8.8
T-1A	Sample **S-2** saturated with TEOS; gelled in HCl; washed; dried at 80 ° C	393	0.45	3.8	-
T-2A	Sample **T-1A** calcined at 560 ° C	1185	1.17	3.8	-
T-1B	Sample **S-2** saturated with TEOS; gelled in NH_4OH; washed; dried at 80 ° C	414	0.54	-	8.8
T-2B	Sample **T-1B** calcined at 560 ° C	169	1.15	2.0	17.2

Experimental

Materials and synthesis procedures

For a quick reference for differences between gels prepared and tested, please see **Table 1**. Composite materials were prepared by saturating spherical, porous, thoroughly water rinsed Amberlite XAD7HP beads from ROHM & HAAS (now Dow Chemical Co.) with 2.7 mol SiO_2/L or 0.5 mol SiO_2/L aqueous, Na/Si ~ 0.76 ratio sodium silicate solution diluted from the commercial STAR$^{®}$ product of PQ Corporation or with 98% pure tetraethoxysilane, TEOS, from Sigma-Aldrich.

The saturated beads were submerged into pH ~ 1 HCl (Na-silicate, TEOS) or pH ~ 11 NH_4OH (TEOS) solutions and kept their overnight. To get base set gel, beads were submerged into so much water that brought the equilibrated overall pH to 7.4 and let it gelling overnight. The gelled composite materials were washed with ion-free water until reaching pH ~ 7 and dried at 80 ^{o}C. A part of these dry composite materials was calcined at 560 ^{o}C to burn out their organic substance. Further details of preparation have been described elsewhere **[15]**.

Instruments and characterization

Scanning Electron Microscopic (SEM) tests were carried out on a FEI Quanta TM 3D FEG microscope operating at 5.0 and 30.0 kV.

Transmission electron microscopy (TEM) tests were carried out on a FEI Titan3™ G2 60-300 operating in high resolution imaging mode at 300.0 kV

Dispersive Raman spectra were measured on a 532 nm RXM spectrometer from Kaiser (~ 180 mW laser power on the sample) using fiber optic connected stainless steel sampling probe capped with sapphire window. Typical sample exposures were about 3 seconds with 30 repetitions. Spectra were baseline corrected, smoothed, and normalized to their most intense bands. With the Q^n connectivity and siloxane ring assignments we followed their averaged values according to reference **[23]**. In the 700-1300 cm^{-1} symmetric and asymmetric Si-O stretching vibration range, which is associated with the Q^n connectivities of the tetrahedral $[SiO_4]$ building blocks of silicates, we employed multiplication factors to compensate for the increasing sensitivity in $Q^4 << Q^1$ direction **[15]**. Therefore the relative intensity of peaks in this region versus those in the < 700 cm^{-1} deformation vibration region is arbitrary.

Porosity measurements were carried out on an ASAP 2405 (Micromeritics, Norcros, GA) volumetric sorption analyzer, using ultrahigh purity N_2 as adsorbate and operating at $p/p_0 \sim 10^{-3}$ to 1 relative pressures. The specific surface area was determined by the BET equation **[24]** and the mesopore size distribution by the BJH method **[25]**. Further experimental details have been described elsewhere **[15, 19, 23]**.

Pore sizes were also measured by positron annihilation lifetime spectroscopy, PALS, using a combined fast-fast (start signal branch) and fast-slow (stop signal branch) delayed coincidence spectrometer **[26]** equipped with scintillation annihilation-radiation detectors with BaF_2 windows. For measurement, a 80 kBq ^{22}Na positron source in a Kapton envelope was placed into the middle of an approximately 4 mm thick layer of the powdered porous

Copyright © 2015 VBRI Press

sample and the whole system was evacuated to 1 x 10^{-5} Pa to remove sorbate molecules from the surface and minimize ortho-para positronium conversion on the paramagnetic oxygen molecules. 1.36 x 10^{6} counts per hour coincidence counting rate and about 2.5 x 10^{7} overall counts were used for each measurement. For further details about PALS see references **[15, 19]**.

Results and discussion

Sodium silicate based gels

Similar to our previously reported swelling effect of TEOS **[15, 19]**, the Amberlite beads got substantially swollen upon saturating them with Na-silicate solutions. This is visible in **Fig. 1**, which also illustrates that the originally white *S-1* Amberlite particles became glassy upon filling them up with the silicate solution (*Na-1*). The pore size distributions in **Fig. 2** attest that the resin pores indeed got saturated in sample *Na-1*. This material was dried at 80 °C, which usually leads to polymerization of the silicate. This dry composite was then calcined at 560 °C to burn out the organic component as we have done on many other occasions **[15, 19]**. One can see in **Fig. 1** that this *Na-2* denoted product consisted of mostly black, deformed and somewhat sintered glassy beads instead of the commonly obtained porous, white silica gel beads when gelling was made from TEOS. **Fig. 2** confirms that *Na-2* is indeed a non-porous glassy material.

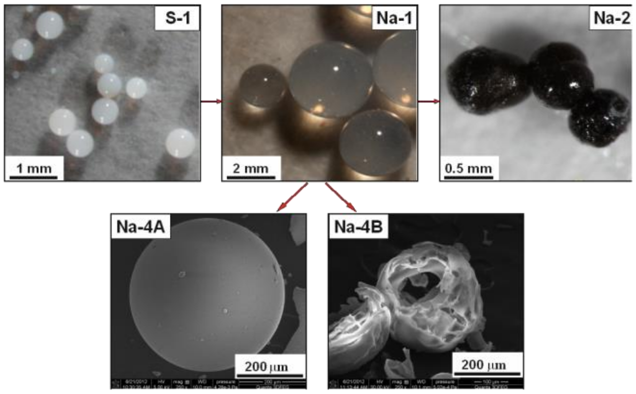

Fig. 1. SEM pictures of the clean, porous Amberlite beads (*S-1*); the same beads after saturating them with Na/Si ~ 0.76 ratio, 2.7 M Na-silicate solution (*Na-1*); after calcining the *Na-1* composite at 560 °C it became *Na-2*; after *Na-1* was treated with HCl, washed with deionized water, and calcined at 560 °C, the *Na-4A* acid set gel was obtained; after *Na-1* was gelled at pH ~7.4, washed with deionized water, and calcined at 560 °C it became *Na-4B* base set gel.

It is reasonable to speculate that glassification took place before the decomposed polymer remnants could leave the silica pores either by evaporation or as gaseous products from combustion. Hence pyrolized carboneous residue is left in these beads. Alkaline silicates have been applied as fire retardants on porous combustibles for over a century **[4, 27]** and the negative effect of alkaline ions on the gel structures have also long been known **[3, 4]**. However, the glass transition temperatures associated with these phenomena usually exceed 650-700 °C **[3, 28, 29]** while we observed Amberlite decomposition beginning at temperatures as low as 250 °C **[15]**. Thus the black glassy appearance of *Na-2* is a bit surprising. For silicates with approximately Na/Si ~ 0.76 ratio, around 400-450 °C glass transition temperature (beginning of softening) has been reported **[30, 31]**. It appears that this leads to pore closing before ignition of the non-volatile organic residues.

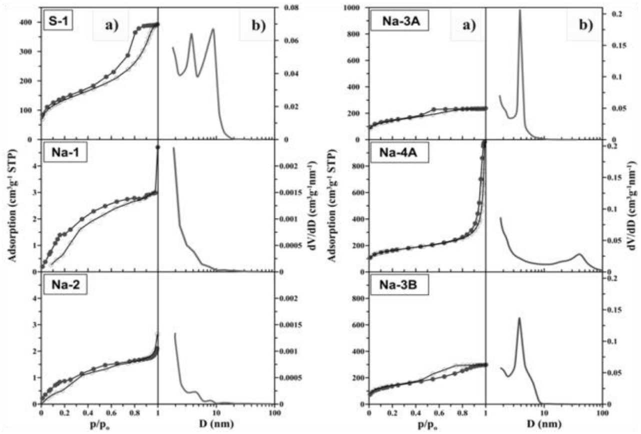

Fig. 2. N_2 sorption isotherms (**a**) and the computed mesopore distribution curves (**b**) of Amberlite/Na silicate composites after various treatments (see **Table 1**).

In our next experiment the *Na-1* silicate/resin composite was exposed to HCl to obtain the acid set *Na-3A* gel composite and it was thoroughly washed with deionized water to minimize its sodium content. In another test the *Na-1* silicate/resin composite was submerged into water, equilibrated to pH ~ 7.4, and kept so overnight for gelling. This *Na-3B* base set gel was then also washed Na-free with deionized water before calcination.

The matching porosity data in **Fig. 2** and **Table 1** indicate that both in *Na-3A* and *Na-3B* the gel fills only the larger resin pores, but itself has no measurable mesopores unless they exactly coincide with the average smaller pore size of Amberlite. The shape of their isotherms (pore saturation at $p/p_0 < 0.1$) suggests that both materials are rather microporous. Despite this similarity in porosity, the 560 °C calcined products of these two acid and base set composite materials are quite different from each other, which is obvious from the SEM pictures in **Fig. 1**. It is likely that the water treatment of *Na-3B* washed out a substantial part of silicate and this resulted in the brittle silica structure of *Na-4B*. We have not tested the porosity of this material. Considering the partial pore filling of *Na-3A*, the smooth spherical shape of *Na-4A* gel is remarkable (**Fig. 1**). According to **Fig. 2**, this acid set gel has mainly macropores in addition to its preserved micropores.

In another series of experiments we repeated the above described gelling procedures with a 0.5 M STAR® solution instead of 2.7 M, to test the potential effect of changing initial molecular composition **[18, 23]**, on the gel properties. **Fig. 3** illustrates that the overwhelmingly Q^2 connected smaller rings in a 3 M STAR® solution transform into larger rings and also some Q^4 connected particles upon dilution coincident with the appearance of a substantial amount of Q^0 monomer silica molecules. Interestingly enough both the microscopic morphology and the porosity properties of products made from the dilute silicate solution resembled quite strongly those made from the 2.7 M starting material. Thus, it seems that the presence of

Amberlite does not affect our earlier observation that the starting composition of alkaline silicates has little effect on the gel structure **[18]**.

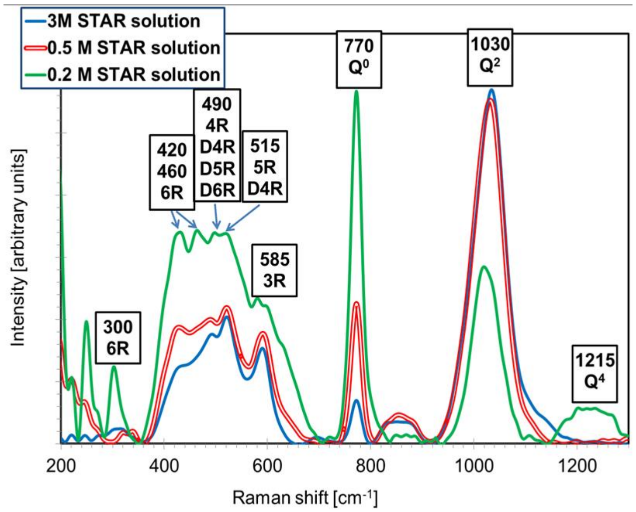

Fig. 3. Effect of dilution on the Raman indicated molecular structures in the Na/Si ~ 0.76 ratio STAR® Na-silicate solution **[18]**. For abbreviation of the rings: 5R = 5 member siloxane ring; D4R = double four siloxane ring; etc.

On the other hand, the molecular structure of differently made silica gels might substantially differ even when the same starting silicate solutions are used **[18, 19, 30]**. This is illustrated in **Fig. 4** (**a**), with the Raman spectra of an acid and a base set gel made from 0.2 M STAR® solution. Note that we employed here the recently found Raman sensitivity factors for getting correct intensity ratios for the Si-O stretching bands associated with the Q^n connectivities **[23]**. It is noteworthy that the base set gel seems to have mostly Q^3 and Q^2 connected [SiO_4] tetrahedra while the acid set gel has mostly Q^4, which is in contrast to most gels tested earlier **[15]**. The reason is not clear at this time. **Fig. 4**(**b**) demonstrates that the molecular structures of acid and base set gels substantially alter when fabricated within the Amberlite pores (for density reasons we used a slightly more concentrated, 0.5 M, STAR solution to saturate the Amberlite pores). It is clear that the earlier described structure directing effect of this porous resin on gels fabricated from TEOS **[15]** (compare **Figs. 8** (**a**) and (**b**) also acts in gels made from the alkaline silicates.

TEOS based gels

We reported recently that gels deposited into Amberlite from TEOS at either acidic or basic conditions maintained the spherical shape of the resin beads and remained porous even after burning out the organic substrate at 550 °C **[15, 19]**. However, the acid set gel resulted in a very smooth bead surface while the base set gel gave a fragmented surface structure as the first two SEM pictures in **Fig. 5** (a) (sample *T-2A*) and **Fig. 5** (b) (sample *T-2B*), respectively illustrate. The matching N_2 sorption isotherms in **Fig. 6** indicate quite different pore structures for these samples, which were also confirmed by their pore size distributions measured by PALS **[19]**. At the substantially increased magnification on the third, TEM, pictures in **Fig. 5** (**a** and **b**) one can see what we believe to be the agglomerated primary colloidal particles that supposedly form at the beginning of polymerization process **[3]**. Interestingly, the plate-like fragmentation of *T-2B* seems to be rooted on the plate-like structure of its primary particles. The unprecedented atomic resolution on the remaining TEM pictures indicates that the morphological and porosity differences of these acid and base set gels are paired with different molecular constitutions just like Raman and ^{29}Si NMR measurements predicted **[15]**.

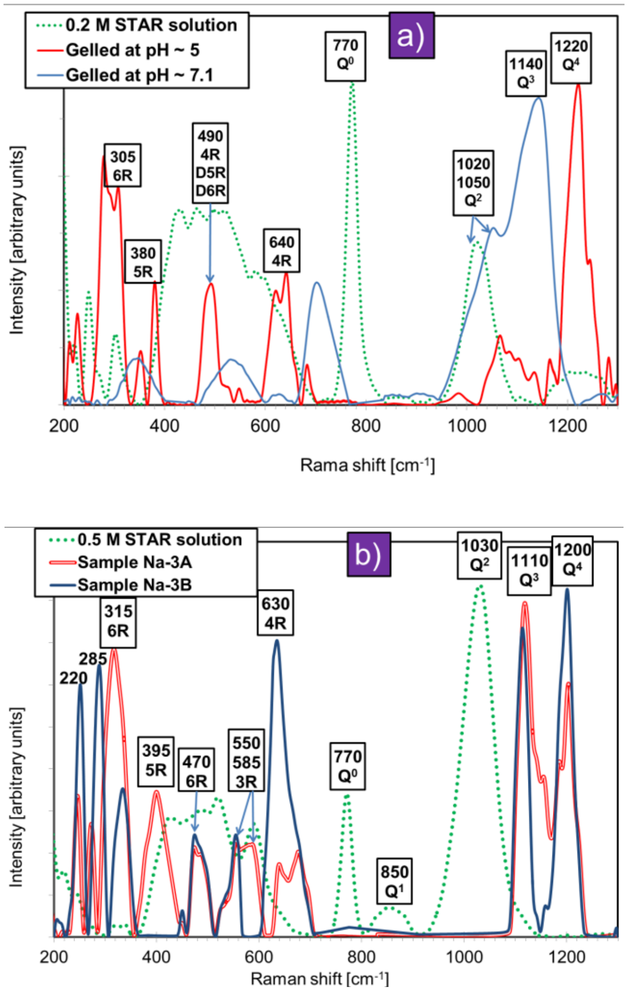

Fig. 4. The Raman spectra of acid and base set gels made from 0.2 M Na/Si ~ 0.76 ratio STAR® Na-silicate solution (a) show characteristic structural differences between each other and also compared to acid and base set gels made from 0.5 M STAR® solution in the structure orienting pores of the Amberlite resin (b) **[18]**.

In line with the pore size data in **Fig. 6**, one can see many 10 to 30 Å size openings on the high resolution TEM photographs of *T-2A* which, according to its Raman spectrum in **Fig. 8**(b), are formed by loosely agglomerated siloxane rings and chains. Presumably this flexible structure allows the smooth macroscopic appearance of this gel surface. In contrast, the high resolution TEM of *T-2B* indicates that most of its atoms are arranged into compact, intercalated siloxane rings, which is in line with their small pore diameters (macropores are not visible on these TEM pictures) and Raman predicted ring structures as shown in **Fig. 6** and **Fig. 8**(b), respectively. Understandably this compact molecular constitution makes this structure rigid, hence fragile.

Copyright © 2015 VBRI Press

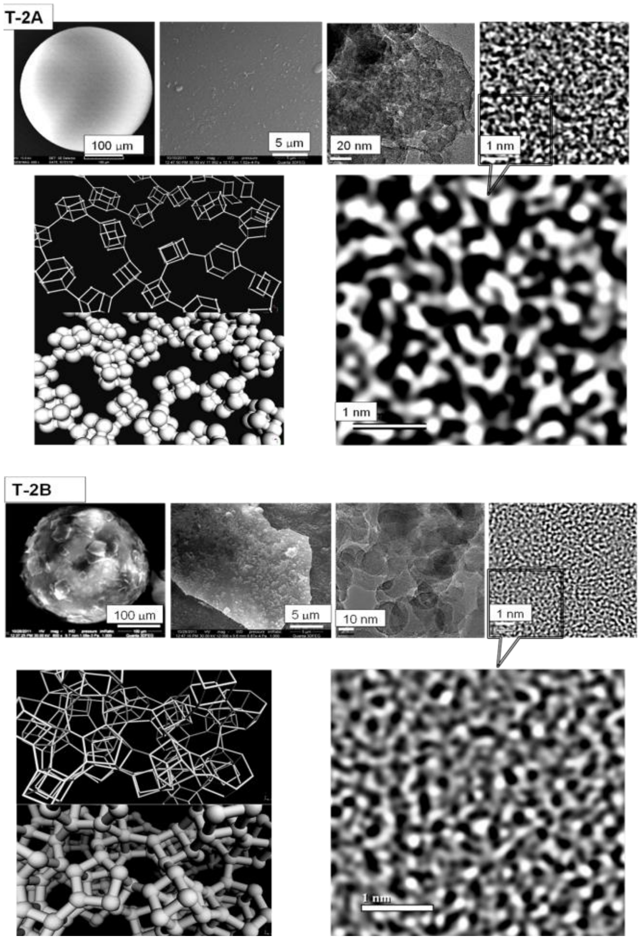

Fig. 5. SEM (at >1 μm) and TEM (at <1 μm) pictures of acid set (**a**) T-2A and base set (**b**) T-2B silica gels made from TEOS in the presence of Amberlite. The lower, "ball and stick", molecular models mimic possible arrangement of the same number of double 4, 5, and 6 member rings in the two gels when their rings are connected via less (T-2A) and more (T-2B) Q^4 connections in accordance with their magnified, atomically resolved pictures. The upper, "line", models are identical with the one below them, but show more clearly how the different rings are interconnected.

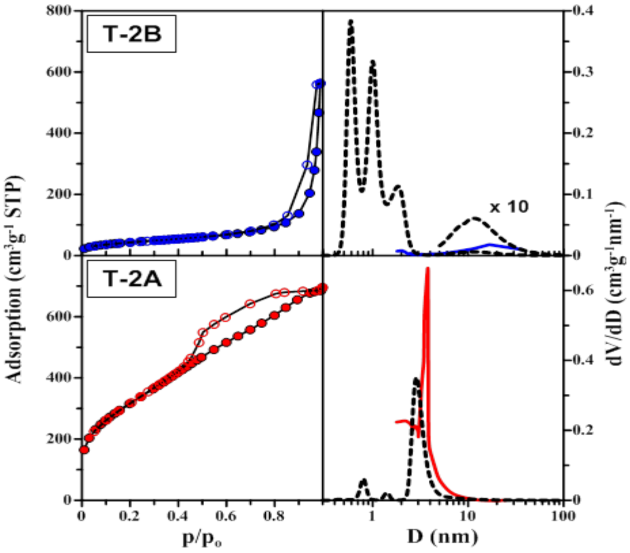

Fig. 6. N_2 sorption isotherm on the acid set T-2A gel indicates presence of mainly meso- and micropores while that on the base set T-2B gel indicates mainly macropores with some micropores. The graphs on the right side show the matching pore size distributions derived from low-temperature N_2 adsorption/desorption data using BJH calculations (solid line) and those measured by the PALS method (dotted line) **[19]**.

For making the atomically resolved TEM pictures in **Fig. 5** more perceptible, we illustrate the real single and double ring structures and the diameters of ring openings in **Fig. 7** assuming an average of 1.7 Å Si-O bond lengths. Also we created a random sequence of the constituting D4R, D5R, and D6R siloxane rings as the Raman spectra in **Fig. 8** (**b**) suggest and connected the same number from these rings according to the different Q^3/Q^4 ratios measured for the acid set *T-2A* and base set *T-2B* gels. These "ball and stick" models are shown side by side with the TEM pictures to mimic the resemblance. Above them their line connected versions are shown to facilitate the visualization of the interconnection of these siloxane rings.

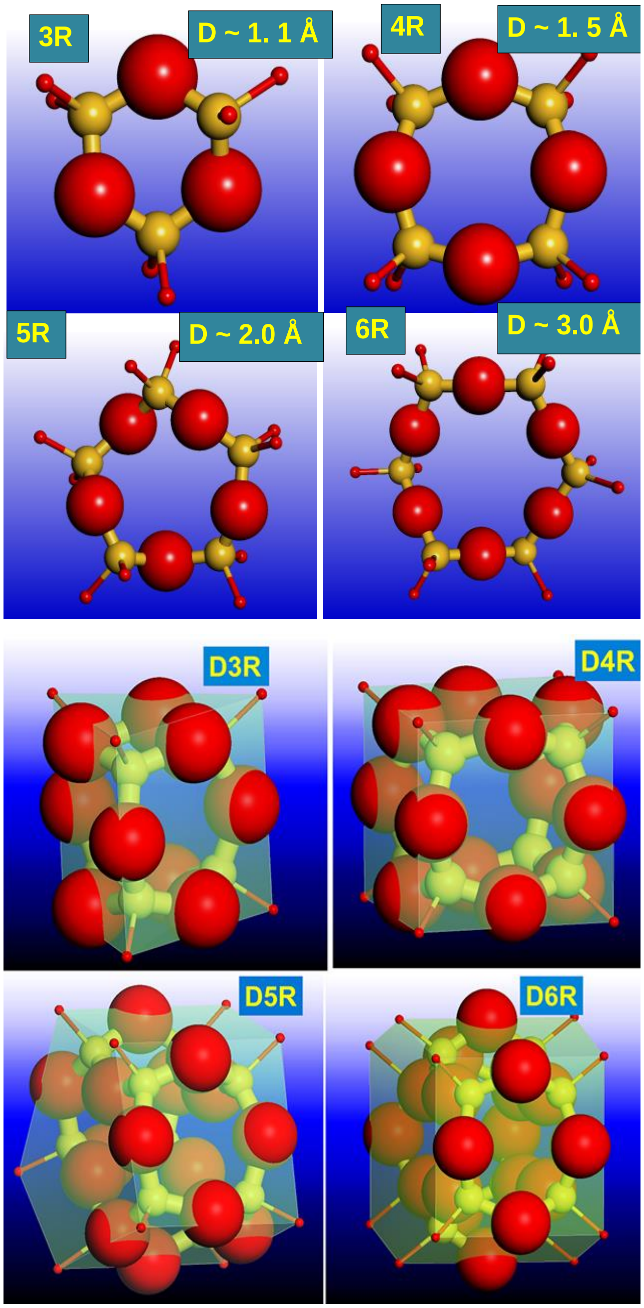

Fig. 7. Realistic space arrangement of atoms (red = oxygen; yellow = silicon) in 3 to 6 member siloxane rings and in the matching double rings. The D opening diameters were calculated to evaluate the opening sizes in the TEM pictures in **Fig. 4**.

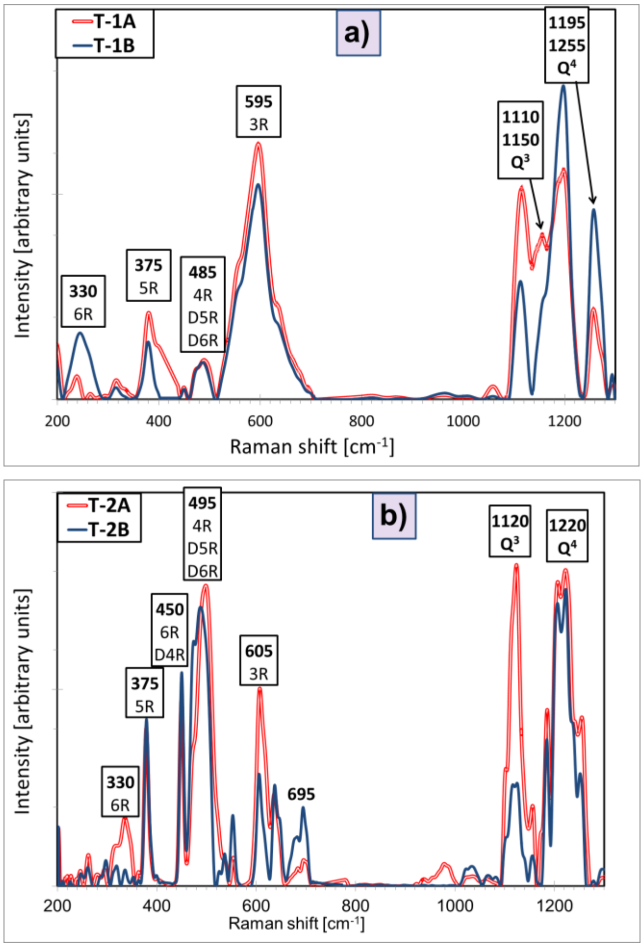

Fig. 8. Raman spectra of the non-calcined acid (T-1A) and base set (T-1B) gels made from TEOS in the Amberlite pores (a) indicate higher Q^3/Q^4 connetivity ratio in the former gel than in the latter one; both structures are different from the gel structures in Fig. 3 (b) made at similar conditions but from Na-silicate. The Raman spectra of their calcined pairs (b) indicate still similar Q^3/Q^4 ratios but significantly increased D4R, D5R, and D6R ring ratios **[15]**.

Conclusion

The morphology and porosity of silica gels prepared from aqueous solutions of a commercial sodium silicate, STAR®, within the pores of a porous organic resin, XAD7HP Amberlite beads, dramatically differ from each other after burning out the organic substance from their structures. Their Raman spectra indicate substantial molecular differences compared to that of gels synthesized without any porous substrate. Thus one can conclude that the porous material exerts a structure directing effect, similar to that observed earlier with TEOS based gels[15] made from non-aqueous solutions. It is also a noteworthy similarity that both the STAR® and the TEOS based gels gave smooth bead surfaces when prepared at acidic conditions and rigid, fragmented surfaces when prepared at basic conditions. These differences are accompanied by different pore sizes in the acid and base set gels. From the here presented and earlier Raman studies combined with ^{29}Si solid state NMR results one can deduce that the different physical properties of gels are paired with molecular differences: the smooth acid set gels have lose, flexible composition of siloxane rings and chains having much Q^3 connected [SiO_4] tetrahedra while the rigid base set gels have a more compact, dense structure mostly with Q^4 connected tetrahedra. The here presented unparalleled atomically resolved TEM pictures let nicely visualize these structural deductions.

All in all, we believe that the present studies convincingly prove that the macroscopic physical parameters of gels depend on their molecular constitution. Thus, designed molecular assembly of siloxane rings can be a chemically controlled route for modifying macroscopic gel properties and/or fabricating new silica gels with desirable physical properties.

Acknowledgements

This research was partly carried out by equipment purchased with the financial support of the European Regional Development Fund in the framework of the Polish Innovation Economy Operational Program (contract no. POIG.02.01.00-06-024/09 Center of Functional Nanomaterials), for which the authors wish to express their gratitude.

Reference

1. Halasz, I. (ed.) *Silica and Silicates in Modern Catalysis*; Transworld Research Network, Kerala, India, **2010.**
ISBN: 978-81-7895-455-4
2. Patterson, R. E. *Surfactant Sci. Ser.* **2006**, *131*, 779.
ISBN: 0-8274-0967-5
3. Iler, R. K. *The Chemistry of Silica*; J. Wiley & Sons, NY, Chichester, Brisbane, Toronto, Singapore, **1979**.
ISBN: 0-471-02404-X
4. Vail, J. G. *Soluble Silicates*; Reinhold Publishing Corp, NY, USA, **1952**. Library of Congress Catalog card Number: 52-8812
5. Wu, Y.; Xue, P.; Kang, Y.; M. Hui; K. M. *Analytical Chemistry* **2013**, *85*, 3166.
DOI: 10.1021/ac303398b
6. Morais, E. C.; Correa, G. G.; Brambilla, R.; Radtke, C.; Baibich, I. M.; dos Santos, J. H. *Z. Colloids and Surfaces, B: Biointerfaces* **2013**, *103*, 422.
DOI: 10.1016/j.colsurfb.2012.10.059
7. Hinestrosa, J. P.; Sutton, J. E.; Allison, D. P.; Doktycz, M. J.; Messman, J. M.; Retterer, S; T. Layer-by-Layer *Langmuir* **2013**, *29*, 2193.
DOI: 10.1021/la3042204
8. Terentyeva, T. G.; Matras, A.; Rossom, W. V.; Hill, J. P.; Ji, Q.; Ariga, K. *J. Mater. Chem. B* **2013**, *1*, 3248.
DOI: 10.1039/c3tb20461h
9. Lai, J.; Shah, B. P.; Garfunkel, E.; Lee, K. *ACS Nano* **2013**, *7*, 2741.
DOI: 10.1021/nn400199t
10. Warren, S. C.; Perkins, M. R.; Adams, A. M.; Kamperman, M.; Burns, A. A.; Arora, H.; Herz, E.; Teeraporn Suteewong, T.; Sai, H.; Li, Z.; Werner, J.; Song, J.; Werner-Zwanziger, U.; Zwanziger, J. W.; Grätzel, M.; DiSalvo, F. J.; Wiesner, U. *Nature Materials* **2012**, *11*, 460.
DOI: 10.1038/nmat3274
11. Gao, L.; Sun, J.; Li, Y *J. Solid State Chem* **2011**, *184*, 1909.
DOI: 10.1016/j.jssc.2011.05.052
12. Zhang, X.; Qian, M.; Zeng, X.; Zhao, Z.; Lasante, J., Plante, P. *J. Sol-Gel Sci. Technol.* **2008**, *45*, 103.
DOI: 10.1007/s10971-007-1635-6
13. Shilova, O. A.; Hashkovsky, S. V.; Tarasyuk, E. V.; Shilov, V. V.; Shevchenko, V. V.; Gomza, Yu. P.; Klimenko, N. S. *J. Sol-Gel Sci. Technol.* **2003**, *26*, 1131.
ISSN: 0928-0707
14. Livage, *J. Stud. Surf. Sci. Catal.* **1994**, *85*, 1.
ISSN: 0167-2991
15. Halasz, I.; Kierys, A.; Goworek, J.; Liu, H.; Patterson, R. E. *J. Phys. Chem. C* **2011**, *115*, 24788.
DOI: 10.1021/jp207534e
16. Depla, A.; Lesthaeghe, D.; van Erp, T. S.; Aerts, A.; Houthoofd, K.; Fan, F.; Li, C., van Speybroeck, V.; Waroquier, M. M.; Kirschhock, C. E.; Martens, J. A. *J. Phys. Chem. C* **2011**, *115*, 3562.
DOI: 10.1021/jp109901v
17. Depla, A.; Verheyen, E.; Veyfeyken, A.; van Houteghem, M.; Houtfold, K.;van Speybroek, V.; Waroquier, M, Kirschhock, C. E.; Martens, J. A.; *J. Phys. Chem. C* **2011**, *115*, 11077.

Copyright © 2015 VBRI Press

DOI: 10.1021/jp200568j

18. Halasz, I.; Agarwal, M.; Patterson, R. E. *Stud. Surf. Sci. Catal*. **2010**, *175*, 209.
    ISSN: 0167-2991
19. Zaleski, R.; Kierys, A.; Dziadosz, M.; Goworek, J.; Halasz, I. *RSC Advances* **2012**, *2*, 3729.
    DOI: 10.1039/c2ra20147j
20. Bunge, F. C. German Patent 523,668, **1931**.
21. Palkin, A. P.; Kolesnikov, A. L. *Zhurn. Prikl. Chim.* **1937**, *10*, 1879.
22. http://www.dow.com/products/market/healthcare-and-medical/product-line/amberlite-xad/product/amberlite-xad-7hp/
23. Halasz, I.; Agarwal, M.; Li, R.; Miller, N. *Microporous Mesoporous Materials* **2010**, *135*, 74.
    DOI: 10.1016/j.micromeso.2010.06.013
24. Brunauer, S.; Emmett, P. H.; Teller, E. *J. Am. Chem. Soc.* **1938**, *60*, 309.
    DOI: 10.1021/ja01269a023
25. Barrett, E. P.; Joyner, L. G.; Halenda, P. P. *J. Am. Chem. Soc.* **1951**, *73*, 373.
    DOI: 10.1021/ja01145a126
26. Hautojarvi, P.; Dupasquier, A. (editors) *Positrons in Solids*, Springer Verlag, Berlin, **1979**.
    ISBN: 978-3-642-81318-4
27. O'Connor, C. H. US Patent 225,858, **1880**.
28. Kim, K. D.; Ondracek, G. *J. Mater. Sci. Lett.* **1995**, *14*, 455.
    ISSN: 0261-8028
29. Akshinskaya, N. V.; Kiselev, A. V.; Nikitin, Yu. S. *Kolloidnyi Zhurnal* **1967**, *29*, 11.
    ISSN: 0023-2912
30. Mysen, B.; Richet, P. *Development in Geochemistry 10, Silicate Glasses and Melts*, Elsevier, Amsterdam, Boston, London, NY, Oxford, Paris, San Diego, San Francisco, Singapore, Sydney, Tokyo, **2005**.
    ISBN: 0444 52011 2
31. Avramov, I.; Vassilev, Ts.; Penkov, I. *J. Non-Crystalline Solids* **2005**, *351*, 472.
    DOI: 10.1016/j.jnoncrysol.2005.01.044

Advanced Materials Letters

Publish your article in this journal

ADVANCED MATERIALS Letters is an international journal published quarterly. The journal is intended to provide top-quality peer-reviewed research papers in the fascinating field of materials science particularly in the area of structure, synthesis and processing, characterization, advanced-state properties, and applications of materials. All articles are indexed on various databases including DOAJ and are available for download for free. The manuscript management system is completely electronic and has fast and fair peer-review process. The journal includes review articles, research articles, notes, letter to editor and short communications.

JOURNAL
VBRI Press
a rapid publication platform